

MEAN-FIELD DENSITY EVOLUTION OF BUNCHED PARTICLES WITH NON-ZERO INITIAL VELOCITY

B. S. Zerbe*, P. M. Duxbury†

Department of Physics and Astronomy, Michigan State University, East Lansing, MI, USA

Abstract

Reed presented a 1D mean-field model of initially cold pancake-beam expansion demonstrating that the evolution of the entire spatial distribution can be solved for all time where the 1D assumption holds. This model is relevant to ultra-fast electron microscopy as it describes the evolution of the distribution within the photoelectron gun, and this model is similar to Anderson's sheet beam density time dependence except that Reed's theory applies to freely expanding beams instead of beams within a focussing channel. Our recent work generalized Reed's analysis to cylindrical and spherical geometries demonstrating the presence of a shock that is seen in the Coulomb explosion literature under these geometries and further discussed the absence of a shock in the 1D model. This work is relevant as it offers a mechanistic explanation of the ring-like density shock that arises in non-equilibrium pancake-beams within the photoelectron gun; moreover, this shock is coincident with a region of high-temperature electrons providing an explanation for why experimentally aperturing the electron bunch results in a greater than 10-fold improvement in beam emittance, possibly even resulting in bunch emittance below the intrinsic emittance of the cathode. However, this theory has been developed for cold-bunches, i.e. bunches of electrons with 0 initial momentum. Here, we briefly review this new theory and extend the cylindrical- and spherical- symmetric distribution to ensembles that have non-zero initial momentum distributions that are symmetric but otherwise unrestricted demonstrating how initial velocity distributions couple to the shocks seen in the less general formulation. Further, we derive and demonstrate how the laminar condition may be propagated through beam foci.

INTRODUCTION

Freely expanding ensembles of charged particles are fundamental to accelerator physics. Although continuous beams near the particle source are relatively diffuse, bunched beams can reach densities where space-charge effects dominate the expansion. In such a regime, the expansion dynamics are similar to the dynamics of Coulomb explosion that are well studied in the laser ablation field, where it is well established that shocks that form at the periphery of the distribution [1–6]. Our group recently found that in an ultrafast electron microscope experimentally aperturing a high density bunch of electrons after they exit the photocathode gun can result in a significant improvement to the brightness. Simulation results suggest that this effect is due to a den-

sity shock, akin to the shock seen in the Coulomb explosion literature, of high-temperature electrons that form at the longitudinal median of the bunch and migrate out to the transverse edge [7].

It has been known for decades that charge redistribution near the particle source is the origin of a major portion of the emittance seen in standard beams [8]. More than 30 years ago, Anderson presented 1D and cylindrical mean-field fluid models of beam dynamics for ensembles of particles with arbitrary initial distributions relevant while the beam remains laminar [9]. These models describe the transverse density and emittance evolution in the presence of a focussing force, and specifically they provide insight into emittance oscillation that is important for emittance compensation [10, 11]. While it is reasonable to make an analogy between that mechanism and the freely expanding charge redistribution we see during Coulomb explosion, Anderson's models are inappropriate for a freely expanding bunch as they assume the focussing force is non-zero and radially inward. Therefore, other models are needed to describe the freely expanding case.

Within the ultrafast electron microscopy (UEM) literature, numerous works postulated 1D models for non-relativistic longitudinal free expansion [12–14], and Reed eventually settled upon the same mean-field fluid approach used by Anderson but without any external fields [15]. Again this model was to describe the longitudinal density evolution of initially dense “pancake” bunches — named so as they have much shorter longitudinal widths than transverse radius — that can be assumed to be planar symmetric instead of Anderson's description of a cylindrical symmetric beam's transverse density evolution. Reed's mean-field model accurately describes the longitudinal expansion while planar symmetry can be assumed [15]. However, Reed was concerned that no Coulomb explosion-like shock was seen in the model even when non-uniform initial conditions were assumed, in stark disagreement to what had been previously found within the Coulomb explosion literature. We recently demonstrated that such a shock cannot occur in the non-relativistic 1D model without careful tuning of the initial velocity distribution [16]. In contrast, we showed that these shocks spontaneously occur in higher dimensions for non-uniform distributions [16], so that the theoretical results found in the UEM community are consistent with the shocks found in the Coulomb explosion literature.

To demonstrate these results, we generalized Reed's model to higher dimension by deriving closed form analytic expressions that describe arbitrary density evolution under cylindrical and spherical symmetries. We discovered that the shocks arise due to relative bunching of particles

* zerbe@pa.msu.edu

† duxbury@pa.msu.edu

that can be described by dimensionally-dependent evolution functions, f_d with $d = 2, 3$ for the cylindrical and spherical symmetric cases, respectively, that are multiplied by the factor $D_{0d} = \frac{d}{2} \left(\frac{\rho_0}{\bar{\rho}_0} - 1 \right)$ where $\rho_0 = \rho_0(r_0)$ and $\bar{\rho}_0 = \bar{\rho}_0(r_0)$ represent the initial probability-like density and initial average probability-like density at r_0 , respectively. D_{0d} is determined entirely from the initial conditions of the distribution, and captures the difference in behavior from that of a uniform distribution, as for the uniform distribution $D_{0d} = 0$. In that case, the density evolution is free from the changes caused by the function f_d and follow a simple power law. We note that most analysis in accelerator physics is based on ensembles with spatially uniform distributions, where the complications introduced by the function f_d are seldom treated analytically, though in many experimental contexts non-uniform distributions are endemic.

As density peaks may arise in the planar symmetric model by carefully tuning the initial velocity distribution, we postulate that the peaks under cylindrical and spherical symmetry should be able to be likewise controlled by the initial velocity distribution. However, our previous model assumes cold initial conditions. Here we present an extension of our previous model that includes arbitrary initial velocities that can be written as a single-value function of the radius of the appropriate symmetry. We demonstrate that this model reproduces particle-in-cell (PIC), implemented in warp [17], simulations. We also show that this model breaks down when an inward velocity that is linear in the radius is assumed for the Gaussian distribution; however, the model correctly predicts the focus and subsequent expansion when a more complicated, non-linear initial velocity profile is assumed.

DERIVATION

In this section, we present a derivation of the density evolution equations with arbitrary initial velocity, $v_0 = v_0(r)$ in the \hat{r} direction, under cylindrical and spherical symmetries. This analysis follows from our earlier work [16] with the following differences: 1) we assume non-zero radial velocity and 2) we adopt slightly modified notation that we have recently developed for a relativistic extension of our initial analysis (un-published).

Consider an ensemble of particles with cylindrical symmetry. Define the time-dependent probability-like density (fraction of entire distribution per unit area), $\rho_2(r, t)$, and denote the initial probability-like density as $\rho_{02} = \rho_{02}(r_0) = \rho_2(r_0, t = 0)$. With the initial conditions, we have,

$$P_{02} = \int_0^{r_0} 2\pi r \rho_{02}(r) dr, \quad E_0(r_0) = E_{02} = \frac{\Lambda_{\text{tot}} P_{02}}{2\pi \epsilon_0 r_0},$$

where Λ_{tot} is the total charge per unit length along the cylindrical charge distribution and P_{02} is the cumulative probability. Notice that the quantity $\Lambda_0 P_{02}$ represents the charge per unit length inside radius r_0 , so further define the average

probabilistic-like density as

$$\bar{\rho}_{02} = \frac{P_{02}}{\pi r_0^2}. \quad (1)$$

Consider an ensemble of particles with spherical symmetry. Define the time-dependent probability-like density (fraction of entire distribution per unit volume), $\rho_3(r, t)$, and denote the initial probability-like density as $\rho_{03} = \rho_{03}(r_0) = \rho_3(r_0, t = 0)$. With the initial conditions, we have,

$$P_{03} = \int_0^{r_0} 4\pi r^2 \rho_{03}(r) dr, \quad E_0(r_0) = E_{03} = \frac{Q_{\text{tot}} P_{03}}{4\pi \epsilon_0 r_0^2},$$

where Q_{tot} is the total charge in the system and P_{03} is the cumulative probability. Again notice that P_{03} represents the fraction of the particles that lie inside radius r_0 and $Q_{\text{tot}} P_{03}$ gives the charge inside radius r_0 , so further define the average probability-like density as

$$\bar{\rho}_{03} = \frac{P_{03}}{\frac{4}{3}\pi r_0^3}. \quad (2)$$

Assuming the distribution undergoes laminar flow, the electric field experienced by a particle at radial position $r(r_0, t)$ under cylindrical and spherical symmetries, respectively, is

$$E_2(r) = E_{02} \frac{r_0}{r}, \quad E_3(r) = E_{03} \left(\frac{r_0}{r} \right)^2.$$

Under the laminar assumption, E_{02} and E_{03} are constants, and the change in potential energy is found by integrating the force qE , and we find,

$$\Delta U_2 = \mathcal{E}_{r2} \ln \left(\frac{r_0}{r} \right), \quad \Delta U_3 = \mathcal{E}_{r3} \left(\frac{r_0}{r} - 1 \right) \quad (3)$$

for the cylindrical and spherical cases respectively. Here $\mathcal{E}_{r2} = \frac{q\Lambda_{\text{tot}} P_{02}}{2\pi \epsilon_0}$ for the cylindrical case and where $\mathcal{E}_{r3} = \frac{qQ_{\text{tot}} P_{03}}{4\pi \epsilon_0 r_0}$ for the spherical case. Notice that by this convention, $\Delta U_d < 0$. Further introduce a fictitious velocity, v_{rd} for $d = 2, 3$, such that $v_{\text{rd}} = +\sqrt{\frac{2\mathcal{E}_{\text{rd}}}{m}}$. Using conservation of energy in the non-relativistic regime with initial energy $\mathcal{E}_0 = \frac{1}{2}mv_0^2$, we can solve for the velocity,

$$\frac{v_2}{v_{r2}} = \pm \sqrt{\frac{\mathcal{E}_0}{\mathcal{E}_{r2}} + \ln \left(\frac{r}{r_0} \right)}, \quad \frac{v_3}{v_{r3}} = \pm \sqrt{\frac{\mathcal{E}_0}{\mathcal{E}_{r3}} + 1 - \frac{r_0}{r}},$$

where the \pm is determined by whether the particle is traveling away or toward the origin and the subscript again indicates the appropriate symmetry. In other words, the velocity equations become double valued for $r < r_0$ when $v_0 < 0$ as both the negative and positive square roots occur; specifically, there is a radius, $r_{\text{td}} < r_0$ with $d = 1, 2$, at which the Lagrangian particle reaches 0 velocity and turns-around, and the velocities between this r_{td} and r_0 are symmetric —

differing only by their sign. By setting $v = 0$, r_{td} can be derived

$$r_{t2} = r_0 e^{-\frac{v_0^2}{v_{r2}^2}}, \quad r_{t3} = \frac{r_0}{1 + \frac{v_0^2}{v_{r3}^2}}. \quad (4)$$

With this notation, the velocities can be rewritten as

$$\frac{v_2}{v_{t2}} = \pm \sqrt{\ln\left(\frac{r}{r_{t2}}\right)}, \quad \frac{v_3}{v_{t3}} = \pm \sqrt{1 - \frac{r_{t3}}{r}}, \quad (5)$$

where $v_{t2} = \sqrt{\frac{q\Lambda_{tot}P_{02}}{\pi m \epsilon_0}} = v_{r2}$ and $v_{t3} = \sqrt{\frac{qQ_{tot}P_{03}}{2\pi m \epsilon_0 r_{t3}}} = v_{r3} \sqrt{\frac{r_0}{r_{t3}}}$. We use these turn-around radii to define the average probability-like densities

$$\bar{\rho}_{t2} = \frac{P_{02}}{\pi r_{t2}^2}, \quad \bar{\rho}_{t3} = \frac{P_{03}}{\frac{4}{3}\pi r_{t3}^3}, \quad (6)$$

and the associated plasma frequencies

$$\omega_{t2} = \sqrt{\frac{q\Lambda_{tot}\bar{\rho}_{t2}}{\epsilon_0 m}} = \frac{v_{t2}}{r_{t2}}, \quad \omega_{t3} = \sqrt{\frac{2}{3}} \sqrt{\frac{qQ_{tot}\bar{\rho}_{t3}}{\epsilon_0 m}} = \frac{v_{t3}}{r_{t3}}, \quad (7)$$

thus effectively mapping this problem to the cold freely-expanding case. The main difference, now, is that r_{td} is a function of both r_0 and v_0 , and ω_{t3} is now a function of both r_0 and v_0 instead of solely r_0 . Furthermore, r_{td} does not necessarily occur at the same time for all Lagrangian particles, so it is not precisely cold expansion-like but is mathematically similar. This will complicate the the derivation of r' where $' \equiv \frac{d}{dr_0}$, but it will much simplify the derivation and interpretation of the time-position relation.

To derive the time-position relation for a specific Lagrangian particle, we consider the normal time-position relation with r_0 replaced by r_{td} . If $v_0 > 0$, then the time-position relation is the same as the cold expansion relations less the time it would take the particle to travel from r_{td} to r_0 , call this t_d for $d = 1, 2$. If $v_0 < 0$, then the particle needs to travel from r_0 to r_{td} before undergoing cold free expansion. As this process is symmetric to the expansion from r_{td} to r_0 , the alteration is again t_{td} . Denote t_{fid} as the portion of the time-position relation defined by the cold free-expansion from r_{td} . Thus, $t = \pm t_{fid} - t_{td}$ where the \pm sign is determined by whether the Lagrangian particle is moving away or toward the origin, respectively, t_d has the same sign as v_0 , and $d = 1, 2$ for the cylindrical and spherical symmetric case, respectively. The parameter t_{fid} can be determined from our previous work:

$$t_{fid} = \frac{2}{\omega_{t2}} e^{y_2^2} F(y_2), \quad (8)$$

$$t_{fid} = \frac{1}{\omega_{t3}} \left(\tanh^{-1} y_3 + \frac{y_3}{1 - y_3^2} \right). \quad (9)$$

where $y_2 = \sqrt{\ln\left(\frac{r}{r_{t2}}\right)}$, $y_3 = \sqrt{1 - \frac{r_{t3}}{r}}$, and $F(\cdot)$ represents the Dawson function. From these equations, we can also obtain t_{td}

$$t_{t2} = \frac{2}{\omega_{t2}} e^{\frac{v_0^2}{v_{r2}^2}} F\left(\frac{v_0}{v_{r2}}\right), \quad (10)$$

$$t_{t3} = \frac{1}{\omega_{t3}} \left(\tanh^{-1} \left(\frac{v_0}{\sqrt{v_0^2 + v_{r3}^2}} \right) + \frac{v_0 \sqrt{v_0^2 + v_{r3}^2}}{v_{r3}^2} \right). \quad (11)$$

Implicit differentiation of t allows us to determine $r' = \frac{dr}{dr_0}$ which is used in the density evolution expression

$$\rho_d(r, t) = \frac{\rho_{0d}}{\left(\frac{r}{r_0}\right)^{d-1} r'}. \quad (12)$$

To obtain an expression for r' , we need to take the derivative of the time with respect to r_0 while holding t constant, and then we solve for r' . We present the results of this process written in terms of time, the ratio $\frac{r}{r_{td}}$, and the initial conditions

$$r' = \begin{cases} -y_d r_{td} \omega_{td} t'_{td} + y_d r_{td} \omega'_{td} t_{fid} + \frac{r}{r_{td}} r'_{td}, & t < -t_{td}, \\ y_d r_{td} \omega_{td} t'_{td} + y_d r_{td} \omega'_{td} t_{fid} + \frac{r}{r_{td}} r'_{td}, & t \geq -t_{td}, \end{cases} \quad (13)$$

for $d = 2, 3$ for the cylindrical and spherical symmetric case, respectively. Notice that all of the derivatives on the right hand side can be written in terms of r_0 , v_0 , v'_0 , and ρ_{0d} ; namely

$$r'_{td} = \frac{r_0^{d-1}}{r_0^{d-1}} \left(1 - 2 \frac{v_0}{v_{rd}} \frac{r_0 v'_0}{v_{rd}} + d \frac{v_0^2}{v_{rd}^2} \frac{\rho_{0d}}{\bar{\rho}_{0d}} \right), \quad (14)$$

$$\omega'_{d3} = \frac{d}{2} \frac{\omega_{td}}{r_0} \left(\frac{\rho_{0d}}{\bar{\rho}_{0d}} - \frac{r_0}{r_{td}} r'_{td} \right), \quad (15)$$

$$t'_{t2} = -\frac{t_{t2}}{\omega_{t2}} \omega'_{t2} + \frac{2}{\omega_{t2}} \frac{v_0}{v_{r2}} e^{\frac{v_0^2}{v_{r2}^2}} \frac{1}{r_0} \left(\frac{r_0 v'_0}{v_0} - \frac{\rho_{02}}{\bar{\rho}_{02}} \right), \quad (16)$$

$$t'_{t3} = -\frac{t_{t3}}{\omega_{t3}} \omega'_{t3} + \frac{1}{\omega_{t3}} \frac{v_0}{v_{r3}} \sqrt{1 + \frac{v_0^2}{v_{r3}^2}} \frac{1}{r_0} \left(1 + 2 \frac{r_0 v'_0}{v_0} - 3 \frac{\rho_{03}}{\bar{\rho}_{03}} \right), \quad (17)$$

so Eq. (13) leads to an analytic form for $\rho_d(r, t)$ through Eq. (12). Note that the condition on the time corresponds to the same \pm condition seen with the velocity and the time-position relation.

COMPARISON TO CYLINDRICALLY-SYMMETRIC SIMULATIONS

We first demonstrate the use of these equation with initially uniform distributions under cylindrical symmetry. Within the initial distribution, we introduce a velocity term that is linear in the initial position, specifically it has the

Content from this work may be used under the terms of the CC BY 3.0 licence (© 2018). Any distribution of this work must maintain attribution to the author(s), title of the work, publisher, and DOI.

form $v_0(r_0) = C \frac{r_0}{R}$ where C is a simulation dependent constant and R is the initial radius of the uniform distribution. This form for the velocity was chosen as it models the linear kick received by a distribution as it passes through a typical focussing lens. For our demonstration, we chose $\Sigma_{\text{tot}} = 2 \times 10^7 \frac{e}{m}$ and $R = 1$ mm, and this corresponds to a $v_{r2} \approx 10^5 \frac{m}{s} \frac{r_0}{R}$. We used the electrostatic Poisson solver in PIC from warp [17] to simulate the evolution of the bunch. Figure 1 shows the results for two values chosen for C , one positive and one negative, both having magnitude equal to the constant associated with v_{r2} . Notice the excellent agreement between theory and simulation in all cases; this is in part due to both the initial velocity and v_{r2} having the same functional form, $\frac{r_0}{R}$, thus the distribution remains laminar.

We next demonstrate the use of these equations with initially Gaussian distributions under cylindrical symmetry. Again we introduce the same initial velocity relation, $v_0(r_0) = C \frac{r_0}{R}$, choosing $\Sigma_{\text{tot}} = 4 \times 10^7 \frac{e}{m}$ and $\sigma_r = 1$ m, which

corresponds to a $v_{r2} \approx 1.4 \times 10^5 \frac{m}{s} \sqrt{1 - e^{-\frac{r_0^2}{2\sigma_r^2}}}$. Unlike the uniform case, the functional form for the initial velocity and the velocity scale differ. As we are interested in the emergence of the shock, we focus our analysis on whether a shock emerges, and if so, the period of time during which the shock emerges. Figure 2 shows the evolution for the three positive values of C . We see that for $C = 10^4 \frac{m}{s}$ the shock emerges around 22 ns instead of the 20 ns emergence seen in the cold case [16]. For $C = 5 \times 10^4 \frac{m}{s}$, the shock is less noticeable and emerges in the vicinity of 50 ns. We do not see the emergence of the shock when $C = 10^5 \frac{m}{s}$ even at times > 100 ns.

Figure 3 shows the evolution for the three negative values of C . We see that for $C = -10^4 \frac{m}{s}$ the shock emerges around 18 ns instead of the 20 ns emergence seen in the cold case, and for $C = -5 \times 10^4 \frac{m}{s}$ the shock seems to emerge in the vicinity of 11 ns although the variation of the simulated density from the theoretical expectation is much larger for this simulation than for the previously investigated simulations. Interestingly, the model predicts qualitatively different behavior than what is seen in simulation for $C = -10^5 \frac{m}{s}$. Specifically, the mean-field fluid model predicts that the distribution begins to expand much earlier than what is seen in simulation. We believe this is due to many Lagrangian particles violating the laminar assumption leading to the incorrect assignment of force to a large proportion of the Lagrangian particles. Specifically, as

$v_0 = C \frac{r_0}{R}$ and $v_{r2} \approx 1.4 \times 10^5 \frac{m}{s} \sqrt{1 - e^{-\frac{r_0^2}{2\sigma_r^2}}}$ results in a the Lagrangian particles mixing as they got to r_{t2} .

To address this concern, we again simulate the cylindrically-symmetric distribution but with $v_0 = C \sqrt{1 - e^{-\frac{r_0^2}{2\sigma_r^2}}}$ for $C < 0$. This velocity profile has the main advantage of $\frac{v_0}{v_{r2}} = \frac{C}{10^5 \frac{m}{s}}$, which is independent of r_0 . This

results in $r_{t2} = \alpha r_0$ where $\alpha = e^{-\frac{c^2}{10^{10} \frac{m^2}{s^2}}}$ where α is indepen-

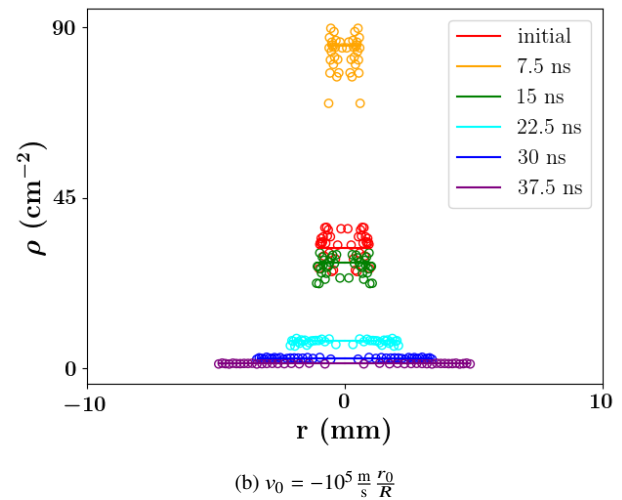
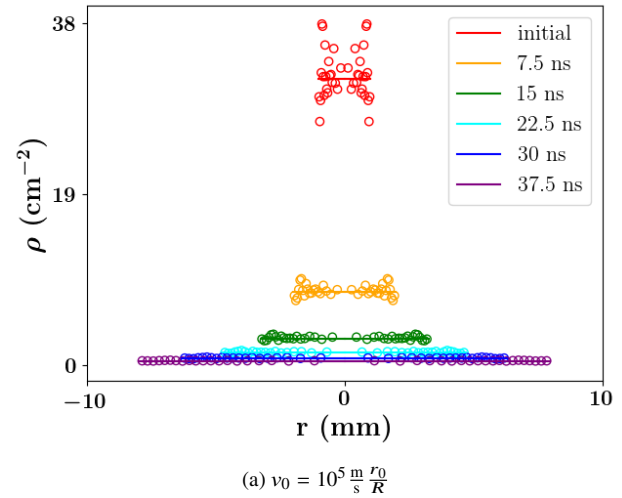


Figure 1: The evolution of uniformly distributed electrons with density of $2 \times 10^7 \frac{e}{m}$ in a $R = 1$ mm radius and where r_0 represent the radial position of the particle. The scale of the initial velocity was chosen to be approximately the same size as the scale of v_{r2} . Solid lines are from the theory presented in this paper and circles are from a single PIC simulation for each figure. Notice that the mean-field fluid model captures the evolution of the bunch in both cases. Specifically, notice that the model correctly captures the contraction and re-expansion of the uniform distribution in the negative case.

dent of r_0 and $t_{t2} = \frac{2\alpha}{\omega_{02}} e^{-\frac{c^2}{10^{10} \frac{m^2}{s^2}}} F\left(\frac{C}{10^5 \frac{m}{s}}\right)$; that is, the turn around points are simply scaled from the initial Gaussian, although they still occur at different times as ω_{02} is still dependent on r_0 . As can be seen in Fig. 4, this distribution does appear to remain laminar through the focus as the theory is now in agreement with simulation when $v_0 > v_{r2}$; however, this comes at a cost of an early-emergence of the shock that can be seen at 10 ns in Fig. 4b.

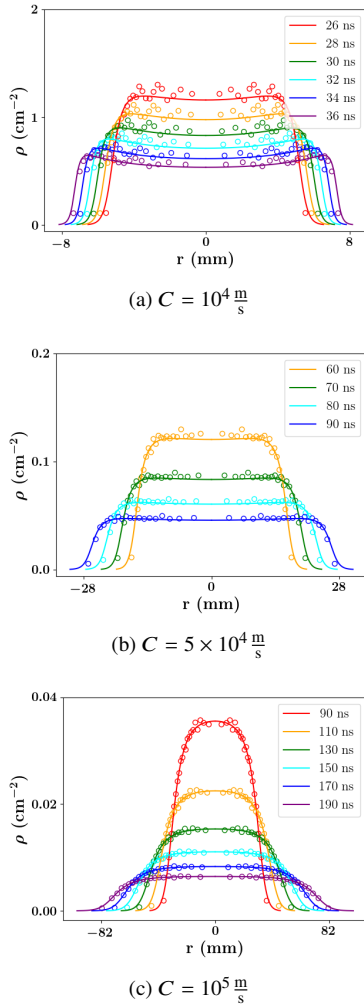


Figure 2: The evolution of Gaussian distributed electrons with density of $4 \times 10^7 \frac{e}{m}$ with $\sigma_r = 1$ mm and with initial velocity of the particle given by $v_0 = C \frac{r_0}{R}$ where r_0 represent the radial position of the particle and $C > 0$. Solid lines are from the theory presented in this paper and circles are from a single PIC simulation for each figure. Notice that the mean-field fluid model captures the evolution of the bunch in all cases. Also notice that large value of C appears to transform the evolution of the bunch into a uniform-like structure and that the bunch apparently loses the emergence of a shock.

COMPARISON TO SPHERICALLY-SYMMETRIC SIMULATIONS

We now demonstrate that the analysis for systems with spherical symmetry is also accurate for a wide range of initial conditions. As for the cylindrical case, we introduce a velocity term that is linear in the initial position, specifically it has the form $v_0(r_0) = C \frac{r_0}{R}$ where C is a simulation dependent constant and R is the initial radius of the uniform distribution. For our demonstration, we chose $Q_{tot} = 2 \times 10^4 e$ and $R = 1$ mm, and this again corresponds

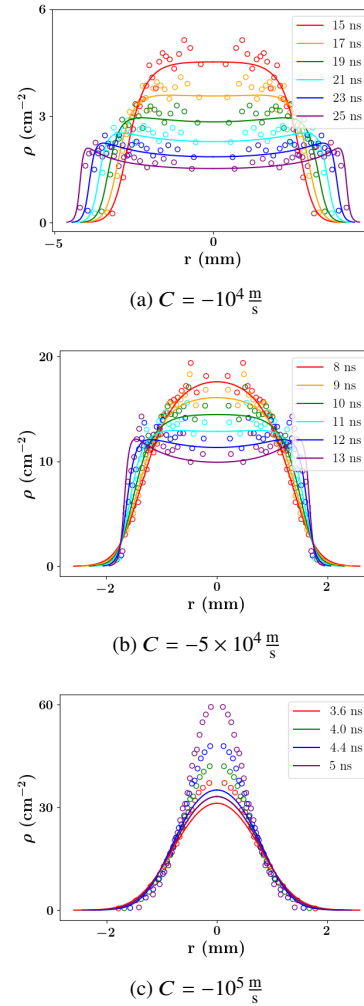


Figure 3: The evolution of Gaussian distributed electrons with density of $4 \times 10^7 \frac{e}{m}$ with $\sigma_r = 1$ mm and with initial velocity of the particle given by $v_0 = C \frac{r_0}{R}$ where r_0 represent the radial position of the particle and $C < 0$. Solid lines are from the theory presented in this paper and circles are from a single PIC simulation for each figure. While the model may be an acceptable approximation for small negative values of C , the mean-field fluid model gets progressively worse as C becomes more negative and provides qualitatively incorrect predictions when $C = -10^5$. The reasons for this are discussed in the text.

to a $v_{r3} \approx 10^5 \frac{m}{s} \frac{r_0}{R}$. We used the electrostatic Poisson solver in PIC from warp [17] to simulate the evolution of the bunch. Figure 5 shows the results for the same two values chosen for C , $\pm 10^5 \frac{m}{s}$, again approximately equal to the constant associated with v_{r3} . Notice the excellent agreement between theory and simulation in all cases thus validating the use of the spherically-symmetric formulation.

CONCLUSIONS

Here, we presented a mean-field fluid model for the evolution of cylindrically and spherically symmetric charged

Content from this work may be used under the terms of the CC BY 3.0 licence (© 2018). Any distribution of this work must maintain attribution to the author(s), title of the work, publisher, and DOI.

Content from this work may be used under the terms of the CC BY 3.0 licence (© 2018). Any distribution of this work must maintain attribution to the author(s), title of the work, publisher, and DOI.

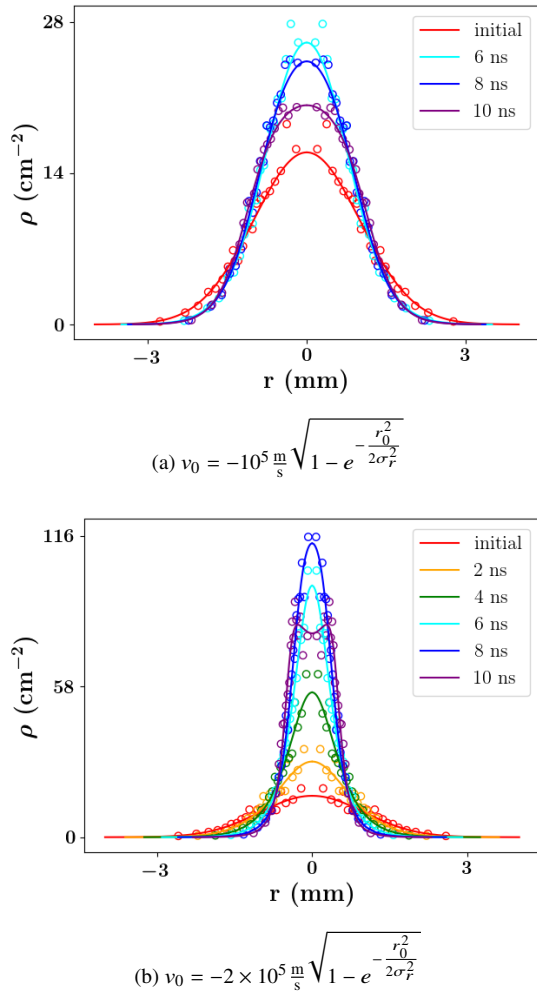


Figure 4: The evolution of Gaussian distributed electrons with density of $4 \times 10^7 \frac{e}{\text{m}^3}$ in a $R = 1 \text{ mm}$ radius and where r_0 represent the radial position of the particle. The functional form of the initial velocity was chosen to be similar to v_{r2} . Solid lines are from the theory presented in this paper and circles are from a single PIC simulation for each figure. Notice that the mean-field fluid model captures the evolution of the bunch in both cases despite the model failing for linear initial velocity of the same scale as seen in Fig. 3. Notice that for (b), a shock emerges between 8 and 10 ns.

bunches with arbitrary initial distribution and initial velocity that can be written as a function of the radial coordinate. We demonstrated that this model predicts the density evolution of the initially uniform bunch when the initial velocity distribution is linear under both spherical and cylindrical geometries. In the cylindrical geometry, we showed that the shock that arises in the cold Gaussian distribution can be suppressed by introducing a initial radially-outward velocity distribution whose linear proportionality constant is of the order or greater than $\sqrt{\frac{q\Lambda_{\text{tot}}}{\pi m \epsilon_0}}$. However, when an analogous negative linear velocity distribution is introduced, the model disagrees with simulations as the initial velocity results in the violation of the laminar assumption. Nonetheless, by

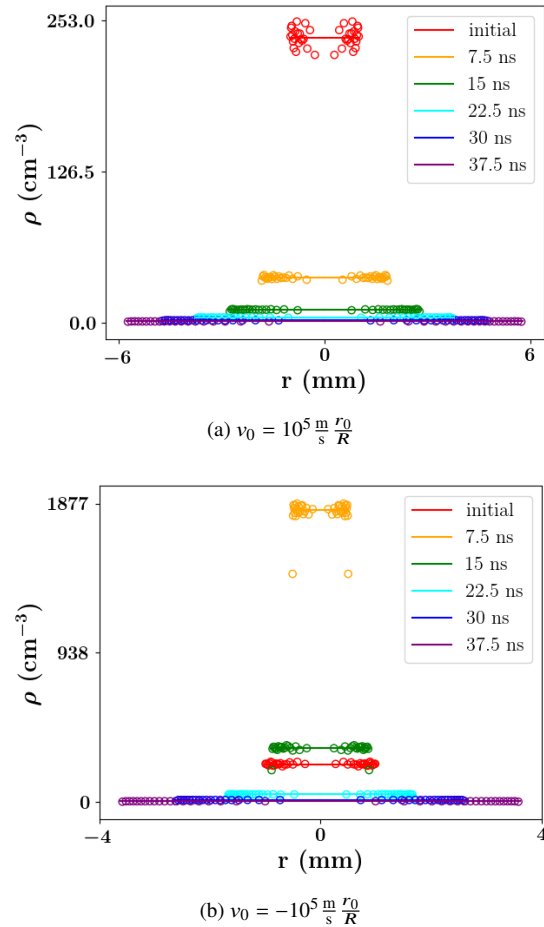


Figure 5: The evolution of uniformly distributed electrons with density of $Q_{\text{tot}} = 2 \times 10^4 e$ with $R = 1 \text{ mm}$ and where r_0 represent the initial radial position of the particle. Solid lines are from the theory presented in this paper and circles are from a single PIC simulation for each figure. Like the cylindrically symmetric case with this initial velocity distribution, notice that the theory is in agreement with the simulations capturing the density of the bunch both as it contracts as well as expands.

adjusting the functional form of the initially velocity distribution from $\frac{r_0}{R}$ to $\sqrt{1 - e^{-\frac{r_0^2}{2\sigma_r^2}}}$, we demonstrated that the model can predict the evolution of the initially Gaussian distribution through the focus including the emergence of a shock. This suggests that the laminar assumption for the Gaussian distribution is not violated by this functional form of the velocity distribution, at least for the duration of time we simulated.

The velocity scales derived in this paper, v_{r2} and v_{r3} , present the means to qualitatively understand when the laminar assumption can be made. For the uniform distribution, $v_{rd} \propto \frac{r_0}{R}$. Thus linear momentum kicks should result in the evolution of the distribution remaining laminar even when the kick is inward; however, if the inward kick has a functional where the slope of the function is beyond linear, say

$v_0 \propto \frac{r_0^2}{R^2}$, outer Lagrangian particle trajectories will cross the trajectories of inner Lagrangian particles and the laminar assumption will be violated. Analogously for the Gaussian

distribution, $v_{rd} \propto \sqrt{1 - e^{-\frac{r_0^2}{2\sigma_r^2}}}$, so it is the slope of this function that matters; that is, the linear kick, where $v_{rd} \propto \frac{r_0}{R}$,

has slope beyond $\sqrt{1 - e^{-\frac{r_0^2}{2\sigma_r^2}}}$ resulting in violation of the

laminar assumption. On the other hand, using $\sqrt{1 - e^{-\frac{r_0^2}{2\sigma_r^2}}}$ as the functional form of the velocity distribution does retain as seen in this work; thus such focussing follows the laminar assumption to the point where the laminar assumption is violated by the shock dynamics as we have discussed in our previous work [16].

In other words, the model we have presented here provides an accurate description of the density evolution of a beam as it expands and focusses as long as the beam dynamics exhibits laminar flow. The model also lends important insight into what parameters drive the beam into non-laminar conditions; specifically shortly after the emergence of a shock and when the focussing kick has a functional form beyond what is needed for the specific distribution. Of course, our theoretical initial distributions are still technically cold as v_0 is exactly specified by r_0 ; however, the initial spatial distribution in the simulations was sampled, and this process does make the beam warm. Despite the beam being warm, though, the model correctly predicts the focussing behavior of both the initially uniform and Gaussian distributions provided that the laminar criteria are met. Presumably there if the temperature is high enough, the model will fail, and an exploration of this condition is one of our current goals; as is extending the analysis presented here to the relativistic regime. The question of whether it is better to remain within this laminar regime or to allow mixing is also worth investigating as we now understand many of the conditions to prevent Lagrangian particle mixing.

ACKNOWLEDGEMENTS

This work was supported by NSF Grant numbers 1803719 and RC108666. Useful discussions with Steve Lund and Chong-Yu Ruan are gratefully acknowledged.

REFERENCES

- [1] M. Grech, R. Nuter, A. Mikaberidze, P. Di Cintio, L. Gremillet, E. Lefebvre, U. Saalman, J. M. Rost, and S. Skupin, "Coulomb explosion of uniformly charged spheroids," *Physical Review E*, vol. 84, no. 5, pp. 056404–056414, 2011.
- [2] A. E. Kaplan, B. Y. Dubetsky, and P. L. Shkolnikov, "Shock shells in coulomb explosions of nanoclusters," *Physical review letters*, vol. 91, no. 14, p. 143401, 2003.
- [3] V. Kovalev and V. Y. Bychenkov, "Kinetic description of the coulomb explosion of a spherically symmetric cluster," *Journal of Experimental and Theoretical Physics*, vol. 101, no. 2, pp. 212–223, 2005.

- [4] I. Last, I. Schek, and J. Jortner, "Energetics and dynamics of coulomb explosion of highly charged clusters," *The Journal of chemical physics*, vol. 107, no. 17, pp. 6685–6692, 1997.
- [5] D. Murphy, R. Speirs, D. Sheludko, C. Putkunz, A. McCulloch, B. Sparkes, and R. Scholten, "Detailed observation of space-charge dynamics using ultracold ion bunches," *Nature communications*, vol. 5, 2014.
- [6] V. P. Degtyareva, M. A. Monastyrsky, M. Y. Schelev, and V. A. Tarasov, "Computer studies on dynamics of ultrashort electron packets in streak tubes and diffractometers," *Optical Engineering*, vol. 37, no. 8, pp. 2227–2232, 1998.
- [7] J. Williams, F. Zhou, T. Sun, K. Chang, K. Makino, M. Berz, P. Duxbury, and C.-Y. Ruan, "Active control of bright electron beams with rf optics for femtosecond microscopy," *Structural Dynamics*, vol. 4, 2017.
- [8] T. P. Wangler, "Emittance growth from space-charge forces," Los Alamos National Lab., NM (United States), Tech. Rep., 1991.
- [9] O. Anderson, "Internal dynamics and emittance growth in space charge dominated beams," *Part. Accel.*, vol. 21, pp. 197–226, 1987.
- [10] L. Serafini and J. B. Rosenzweig, "Envelope analysis of intense relativistic quasilaminar beams in rf photoinjectors: ma theory of emittance compensation," *Physical Review E*, vol. 55, no. 6, p. 7565, 1997.
- [11] J. Rosenzweig, A. Cook, R. England, M. Dunning, S. Anderson, and M. Ferrario, "Emittance compensation with dynamically optimized photoelectron beam profiles," *Nuclear Instruments and Methods in Physics Research Section A: Accelerators, Spectrometers, Detectors and Associated Equipment*, vol. 557, no. 1, pp. 87–93, 2006.
- [12] O. J. Luiten, S. B. vanderGeer, M. J. deLoos, F. B. Kiewiet, and M. J. vanderWiel, "How to realize uniform three-dimensional ellipsoidal electron bunches," *Physical review letters*, vol. 93, no. 9, p. 094802, 2004.
- [13] B. J. Siwick, J. R. Dwyer, R. E. Jordan, and R. J. Dwayne Miller, "Ultrafast electron optics: Propagation dynamics of femtosecond electron packets," *Journal of Applied Physics*, vol. 92, no. 3, pp. 1643–1648, 2002.
- [14] B.-L. Qian and H. E. Elsayed-Ali, "Electron pulse broadening due to space charge effects in a photoelectron gun for electron diffraction and streak camera systems," *Journal of Applied Physics*, vol. 91, no. 1, pp. 462–468, 2002.
- [15] B. W. Reed, "Femtosecond electron pulse propagation for ultrafast electron diffraction," *Journal of Applied Physics*, vol. 100, no. 3, pp. 034916–034931, 2006.
- [16] B. Zerbe, X. Xiang, C.-Y. Ruan, S. Lund, and P. Duxbury, "Dynamical bunching and density peaks in expanding coulomb clouds," *Physical Review Accelerators and Beams*, vol. 21, no. 6, p. 064201, 2018.
- [17] A. Friedman, R. H. Cohen, D. P. Grote, S. M. Lund, W. M. Sharp, J.-L. Vay, I. Haber, and R. A. Kishek, "Computational methods in the warp code framework for kinetic simulations of particle beams and plasmas," *IEEE Transactions on Plasma Science*, vol. 42, no. 5, pp. 1321–1334, 2014.